Electronic Supplementary Information

Copper(II)-mediated base pairing involving the artificial nucleobase 3H-imidazo[4,5-f]quinolin-5-ol

Nikolas Sandmann,[a] Jim Bachmann,[b] Alexander Hepp,[a] Nikos L. Doltsinis[b] and Jens Müller*[a]*

a) Westfälische Wilhelms-Universität Münster, Institut für Anorganische und Analytische Chemie, Corrensstr. 28/30, 48149 Münster, Germany. E-mail: mueller.j@uni-muenster.de

b) Westfälische Wilhelms-Universität Münster, Institut für Festkörpertheorie and Center for Multiscale Theory and Computation, Wilhelm-Klemm-Straße 10, 48149 Münster, Germany. E-Mail: nikos.doltsinis@uni-muenster.de

1) Experimental data

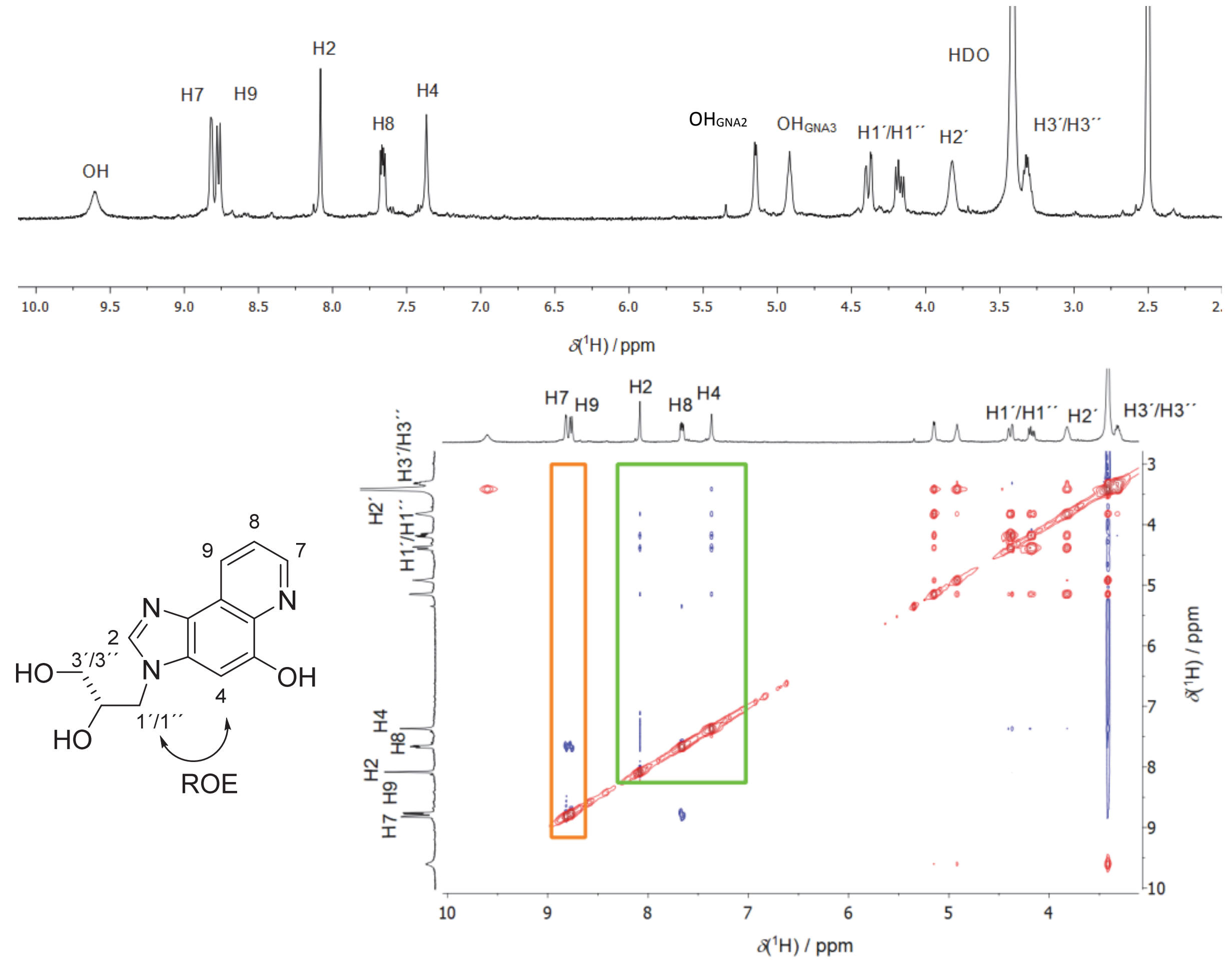

Fig. S1 ^{1}H NMR (top) and ^{1}H,^{1}H-ROESY NMR spectra of compound **1** in DMSO-*d*$_6$. Formation of the desired regioisomer with binding of the propylene glycol unit to the N3 position of the ligand can clearly be derived from the numerous cross-peaks involving the H2 and H4 atoms of the ligand and the propylene glycol hydrogen atoms (green box), whereas no such cross-peaks are observed for the H9 atom of the ligand (orange box).

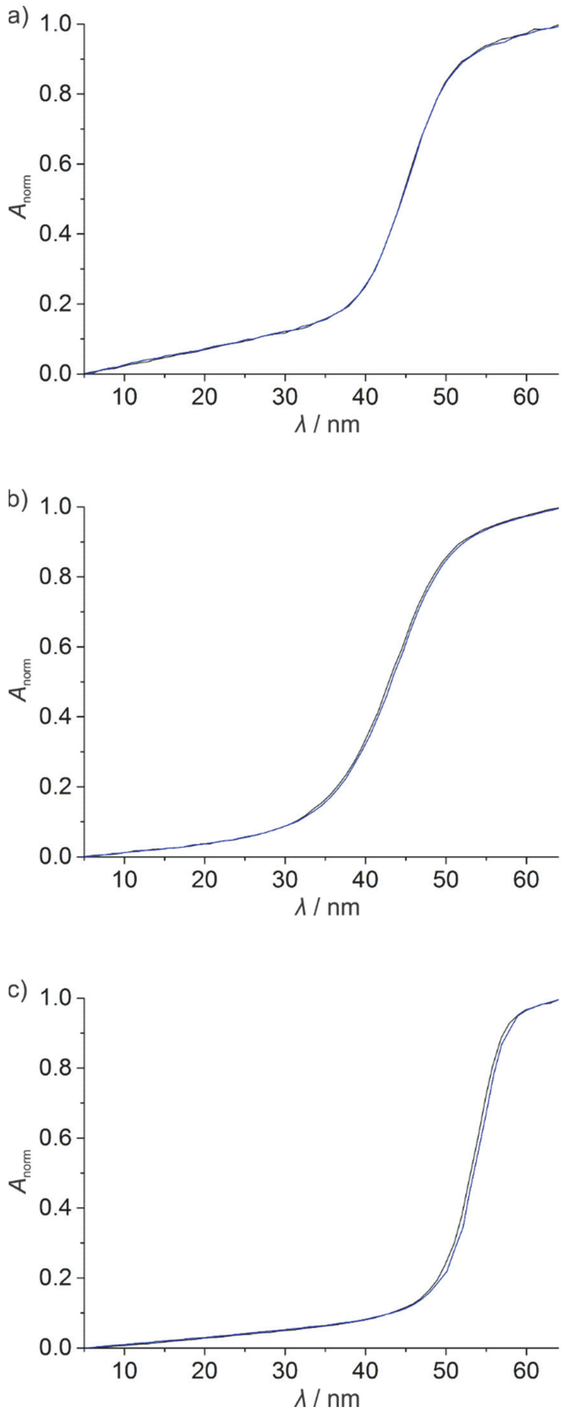

Fig. S2 Melting curves of duplexes a) $\mathbf{I_{ref}}$, b) $\mathbf{II_{ref}}$ and c) $\mathbf{III_{ref}}$ in the absence (black) and presence (blue) of one equiv. of Cu(II) Experimental conditions: 1 μM duplex, 150 mM $NaClO_4$, 5 mM CHES (pH 10.0).

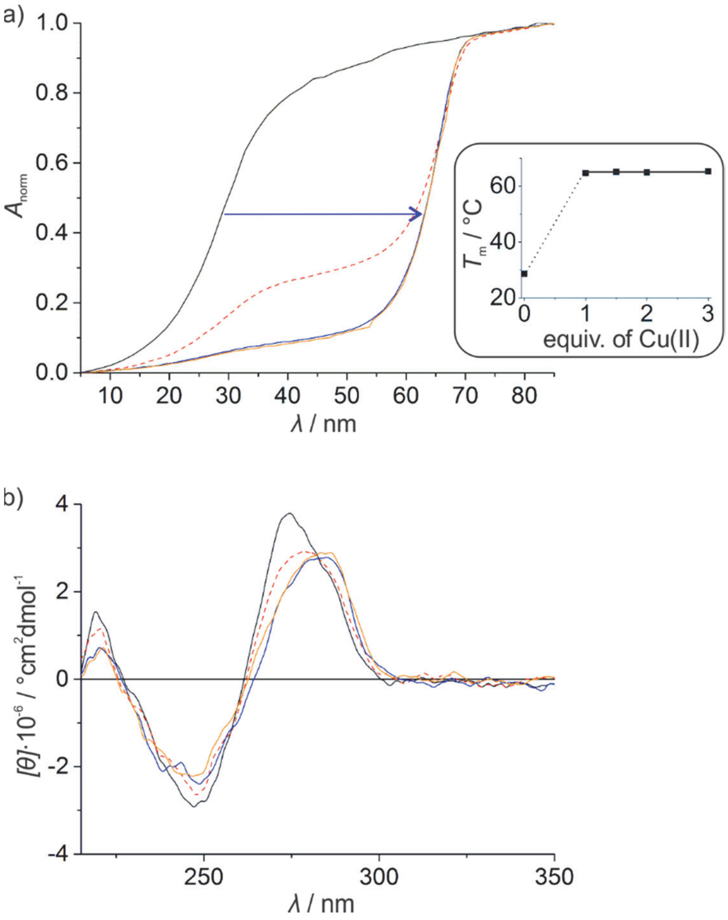

Fig. S3 a) Melting curves and b) CD spectra of duplex **IIa** in the presence of increasing amounts of Cu(II) (black: no Cu(II), red: 0.5 equiv. of Cu(II), blue: 1 equiv. of Cu(II), orange: 2 equiv. of Cu(II)). The inset shows the increase in melting temperature T_m upon the addition of Cu(II). Experimental conditions: 1 μM duplex, 150 mM $NaClO_4$, 5 mM CHES (pH 10.0).

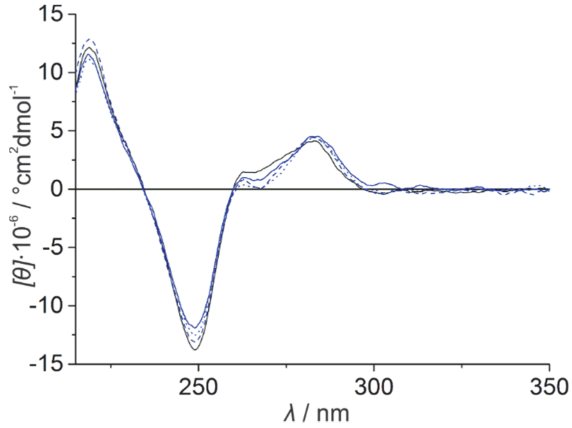

Fig. S4 CD spectra of duplex **IIIa** in the absence (black) and presence (blue) of one Cu(II) per duplex (solid line: after 7 d, broken line: after 14 d, dotted line: after 21 d). Experimental conditions: 1 μM duplex, 150 mM $NaClO_4$, 5 mM CHES (pH 10.0).

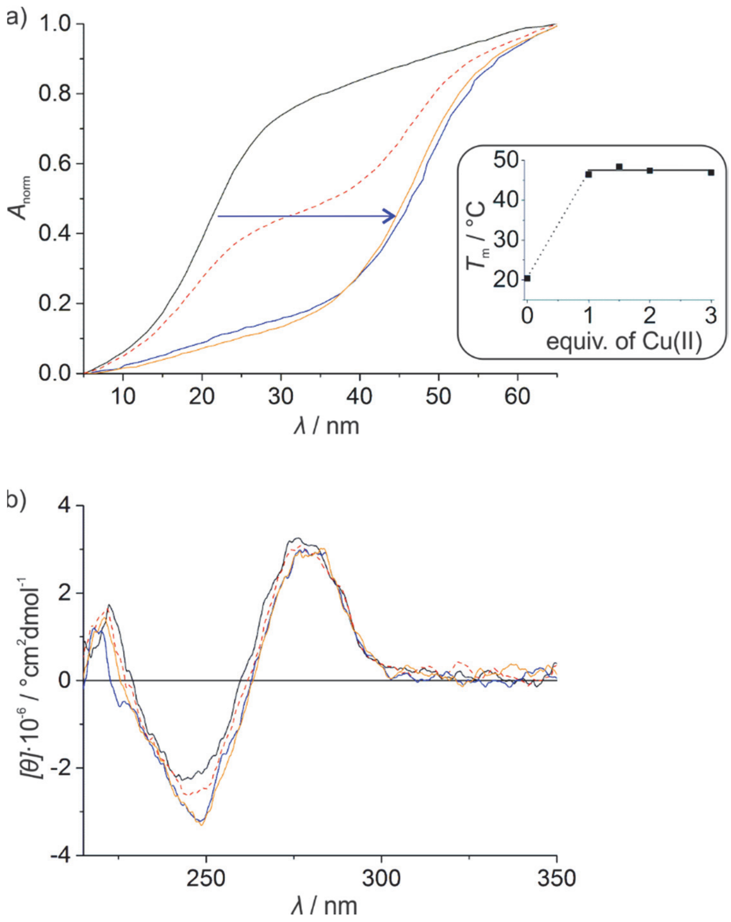

Fig. S5 a) Melting curves and b) CD spectra of duplex **Ib** in the presence of increasing amounts of Cu(II) (black: no Cu(II), red: 0.5 equiv. of Cu(II), blue: 1 equiv. of Cu(II), orange: 2 equiv. of Cu(II)). The inset shows the increase in melting temperature T_m upon the addition of Cu(II). Experimental conditions: 1 μM duplex, 150 mM $NaClO_4$, 5 mM CHES (pH 10.0).

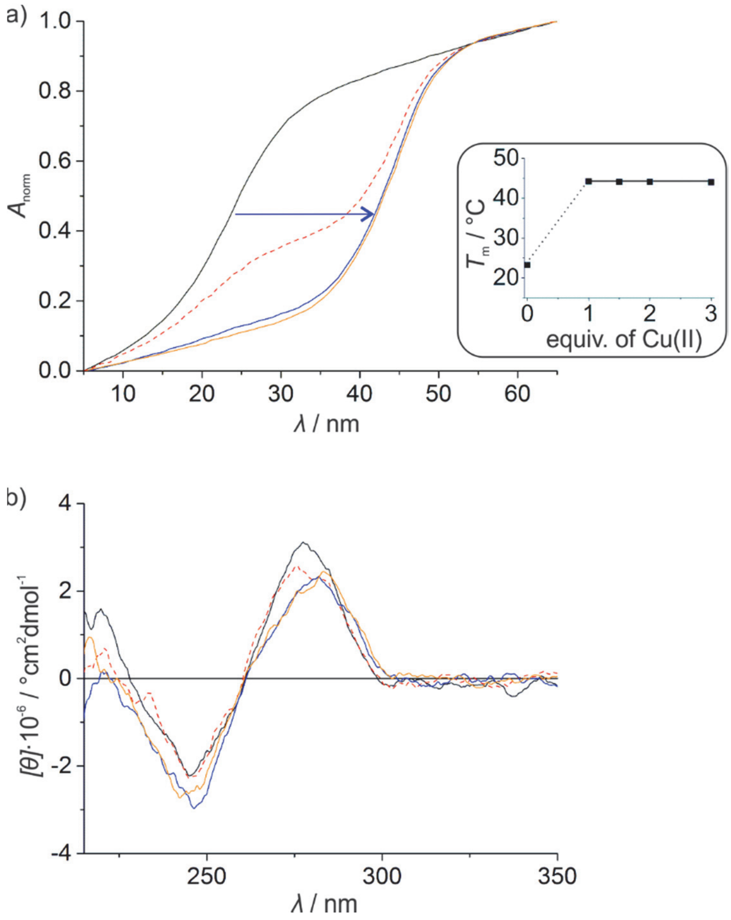

Fig. S6 a) Melting curves and b) CD spectra of duplex **Ic** in the presence of increasing amounts of Cu(II) (black: no Cu(II), red: 0.5 equiv. of Cu(II), blue: 1 equiv. of Cu(II), orange: 2 equiv. of Cu(II)). The inset shows the increase in melting temperature T_m upon the addition of Cu(II). Experimental conditions: 1 μM duplex, 150 mM $NaClO_4$, 5 mM CHES (pH 10.0).

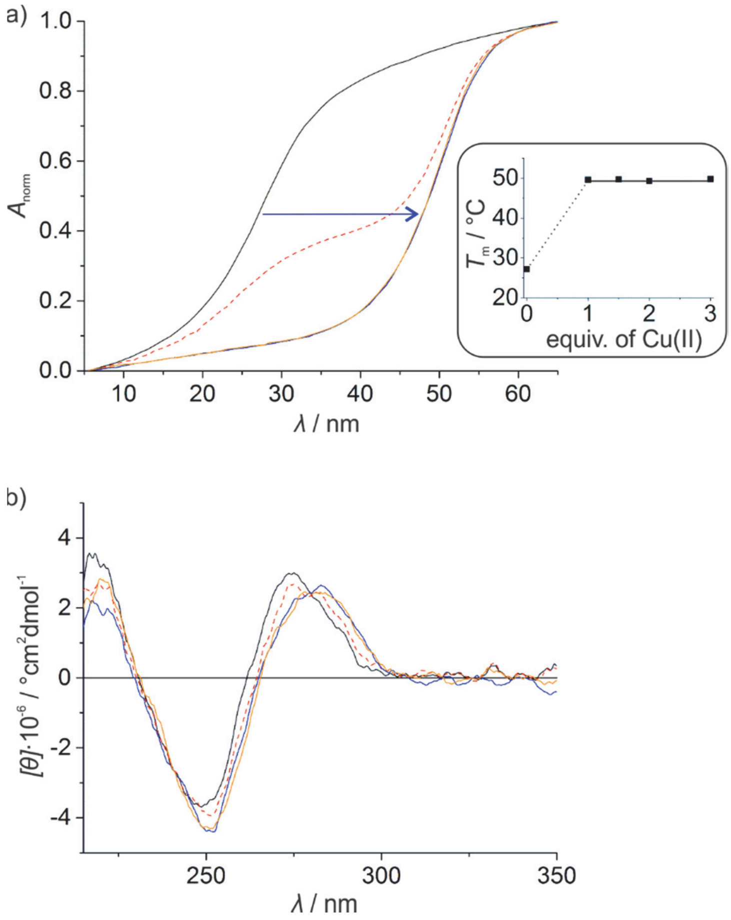

Fig. S7 a) Melting curves and b) CD spectra of duplex **IIb** in the presence of increasing amounts of Cu(II) (black: no Cu(II), red: 0.5 equiv. of Cu(II), blue: 1 equiv. of Cu(II), orange: 2 equiv. of Cu(II)). The inset shows the increase in melting temperature T_m upon the addition of Cu(II). Experimental conditions: 1 μM duplex, 150 mM $NaClO_4$, 5 mM CHES (pH 10.0).

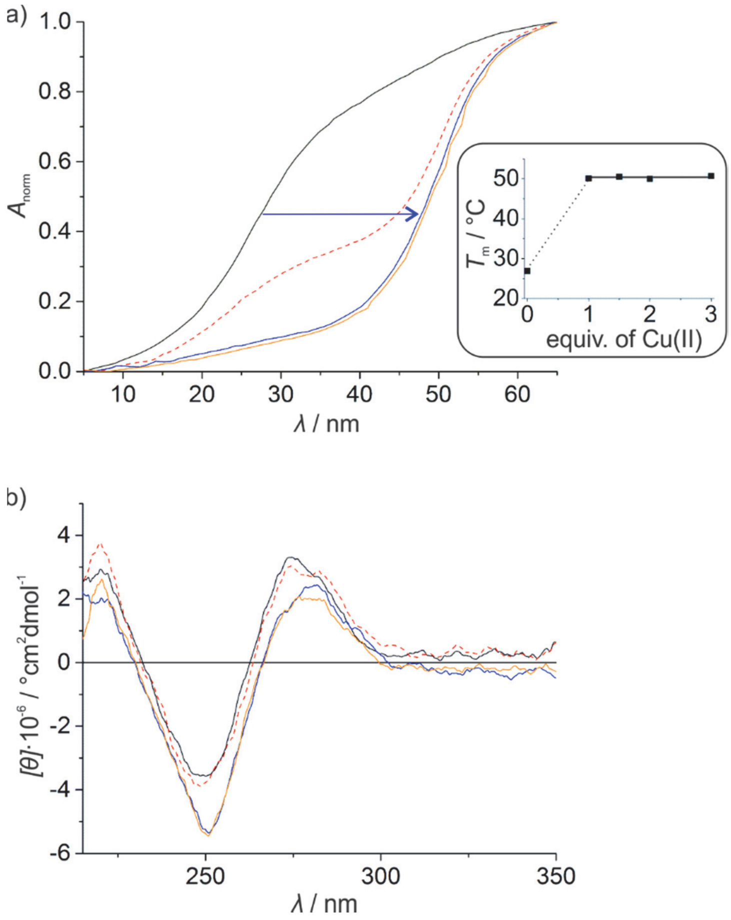

Fig. S8 a) Melting curves and b) CD spectra of duplex **IIc** in the presence of increasing amounts of Cu(II) (black: no Cu(II), red: 0.5 equiv. of Cu(II), blue: 1 equiv. of Cu(II), orange: 2 equiv. of Cu(II)). The inset shows the increase in melting temperature T_m upon the addition of Cu(II). Experimental conditions: 1 μM duplex, 150 mM $NaClO_4$, 5 mM CHES (pH 10.0).

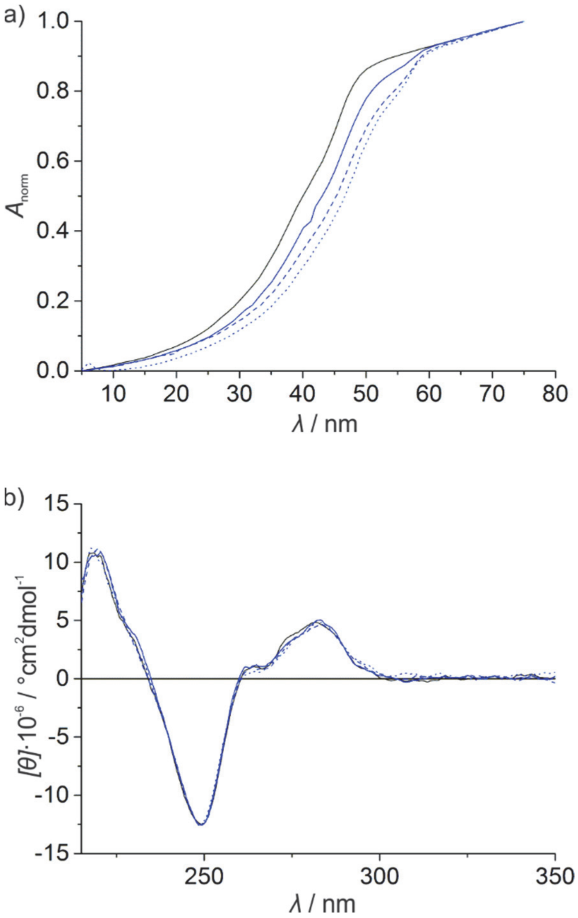

Fig. S9 a) Melting curves and b) CD spectra of duplex **IIIb** in the absence (black) and presence (blue) of one Cu(II) per duplex (solid line: after 7 d, broken line: after 14 d, dotted line: after 21 d). Experimental conditions: 1 μM duplex, 150 mM $NaClO_4$, 5 mM CHES (pH 10.0).

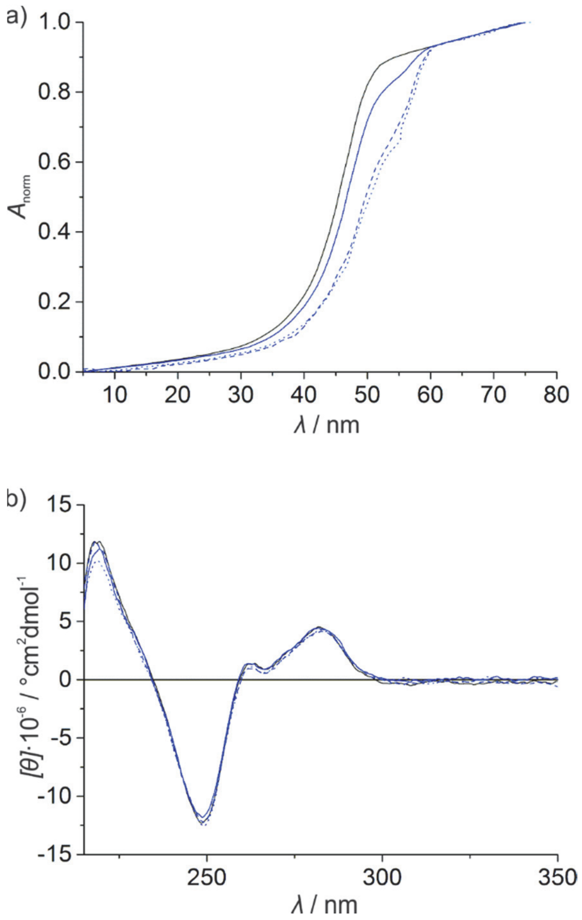

Fig. S10 a) Melting curves and b) CD spectra of duplex **IIIc** in the absence (black) and presence (blue) of one Cu(II) per duplex (solid line: after 7 d, broken line: after 14 d, dotted line: after 21 d). Experimental conditions: 1 μM duplex, 150 mM $NaClO_4$, 5 mM CHES (pH 10.0).

Table S1 Mass-spectrometric characterization of the oligonucleotides.[a]

Oligonucleotide	Molecular formula (M)	$(M+H)^+$ / Da	
		Calcd.	Found
ODN1	$C_{133}H_{159}N_{57}O_{73}P_{12}$	4095	4096
ODN2	$C_{127}H_{161}N_{39}O_{77}P_{12}$	3837	3837
ODN7	$C_{151}H_{187}N_{51}O_{89}P_{14}$	4573	4575
ODN8	$C_{151}H_{185}N_{57}O_{85}P_{14}$	4591	4594
ODN13	$C_{263}H_{334}N_{65}O_{174}P_{25}$	7961	7964
ODN14	$C_{259}H_{313}N_{120}O_{132}P_{25}$	7990	7993

[a] **1** = Artificial nucleoside analogue based on 3*H*-imidazo[4,5-*f*]quinolin-5-ol. The synthesis and characterization of the oligonucleotides containing nucleoside **2** (ODN3, ODN4, ODN9, ODN10, ODN15 and ODN16) and of the reference duplexes (ODN5, ODN6, ODN11, ODN12, ODN17, ODN18) have been reported before.[1]

2) Theoretical determination of pK_a values

2.1) Constrained AIMD simulations

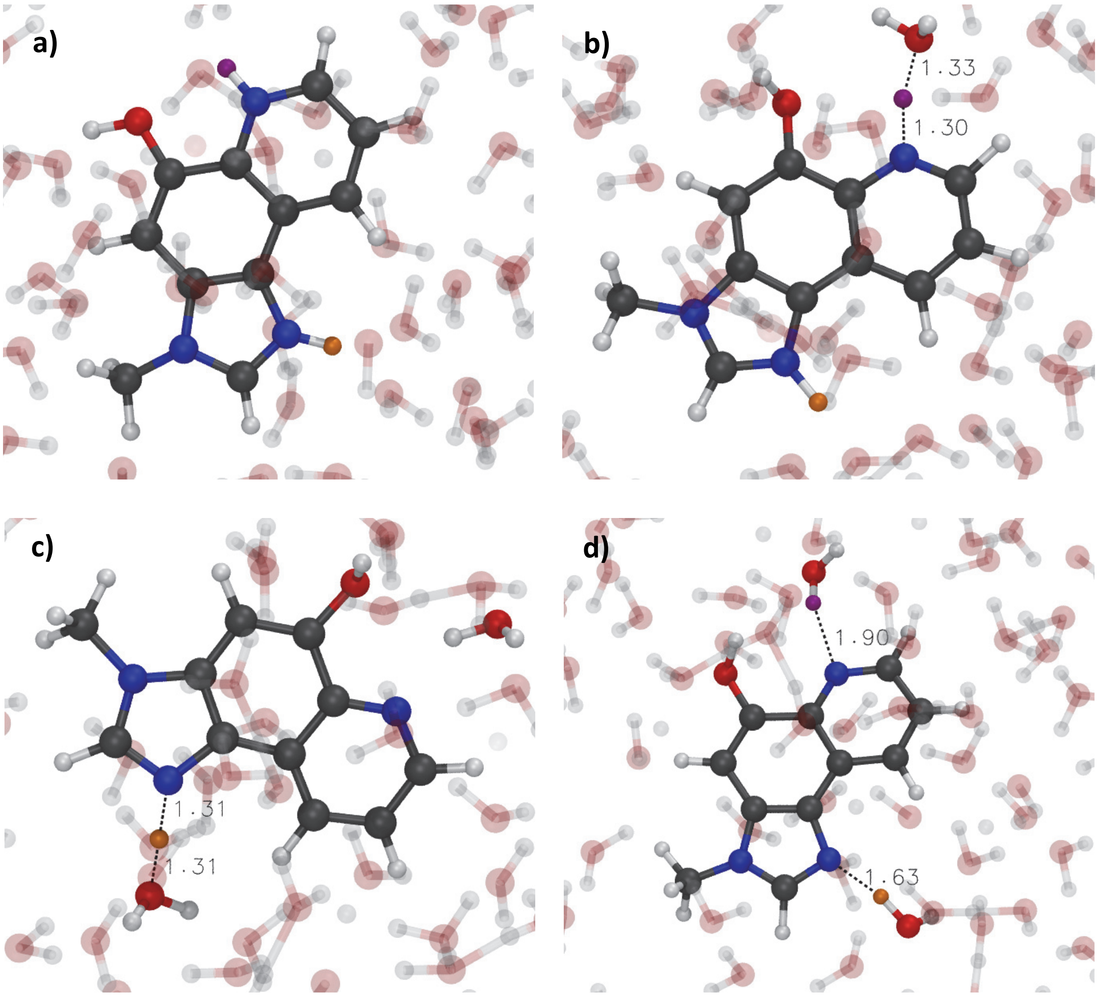

Fig. S11. Snapshots of the AIMD simulation of doubly protonated **1**. The dissociating hydrogen atoms are coloured purple (site A) and orange (site B), all other hydrogen atoms are coloured white, carbon atoms grey, nitrogen atoms blue, and oxygen atoms red. (a) Initial structure at n = 1. (b) Transition state for deprotonation of site A at n = 0.8. (c) Transition state for deprotonation of site B at n = 0.4. (d) Doubly deprotonated state at n = 0.15.

Table S2. pK_a values of initially doubly protonated **1** obtained from constrained AIMD simulations by thermodynamic integration. A_A refers to A being deprotonated while site B remains protonated, A_B refers to A being deprotonated after site B has been deprotonated, B_B refers to B being deprotonated while site A remains protonated, B_A refers to B being deprotonated after site A has been deprotonated.

Site	**protonation state**	**r_c [Å]**	**r_{max} [Å]**	**K_a**	**pK_a**
A_B	1+	1.3	1.6	1.28×10^{-5}	4.9
A_A	2+	1.3	1.6	1.90×10^{-3}	2.7
B_A	1+	1.3	1.6	1.80×10^{-6}	5.7
B_B	2+	1.3	1.6	6.58×10^{-3}	2.2

Table S3. pK_a values of initially singly protonated **1** obtained from constrained AIMD simulations by thermodynamic integration.

Site	**protonation state**	**r_c [Å]**	**r_{max} [Å]**	**K_a**	**pK_a**
A	1+	1.3	1.6	9.58×10^{-7}	6.0

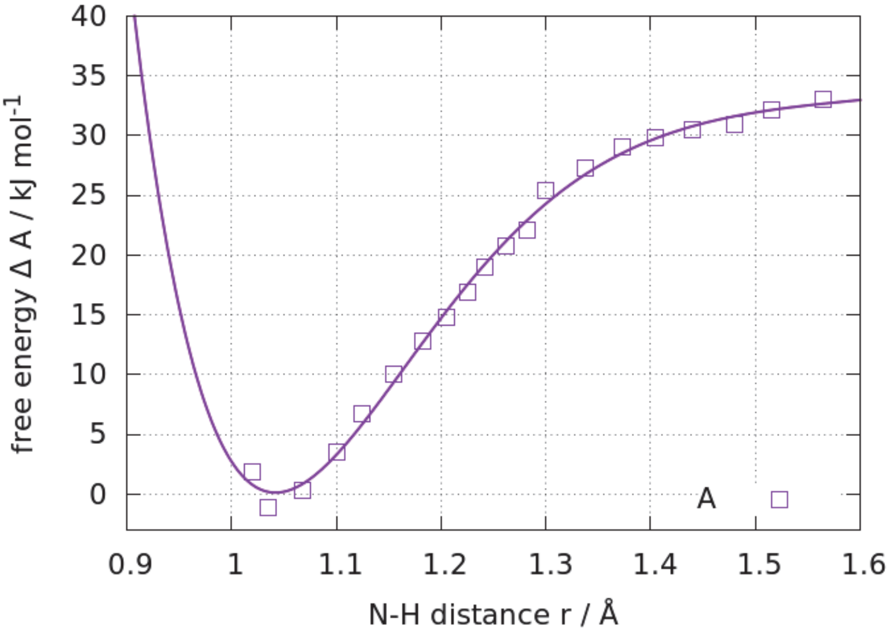

Fig. S12. Change in free energy against N–H distance for singly protonated **1** at site A. The solid lines represent the fitted functions for numerical integration. The minimum of the free energy profile was set to zero.

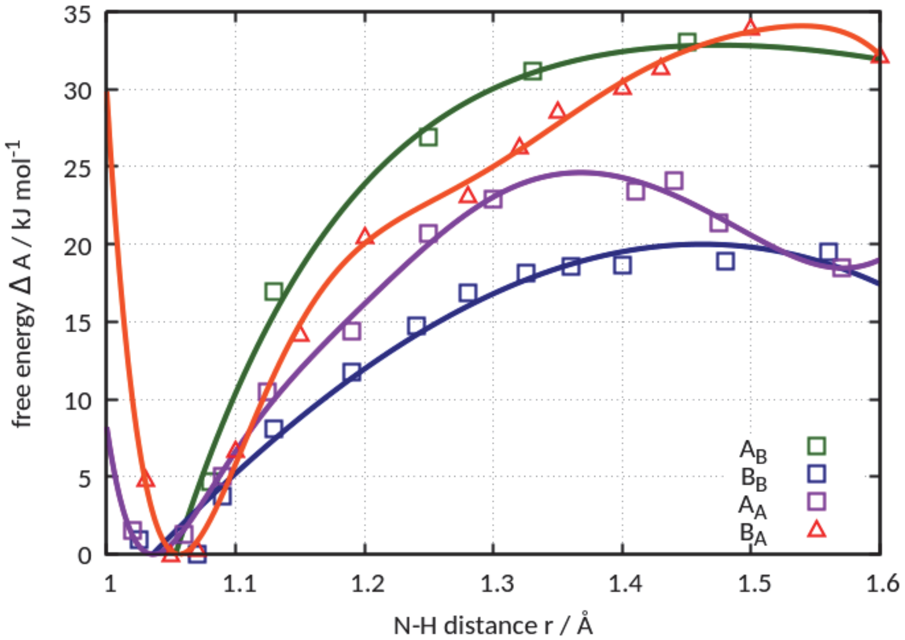

Fig. S13. Change in free energy against N-H distance for initially doubly protonated **1** for sites A and B from two different simulations. In one simulation, site A is deprotonated before B (curves A_A and B_A), while in the other site B is deprotonated before A (curves A_B and B_B). The subscript denotes which site deprotonated first. The lines represent the fitted functions for numerical integration. The minima of the free energy profile were set to zero for each dissociation separately.

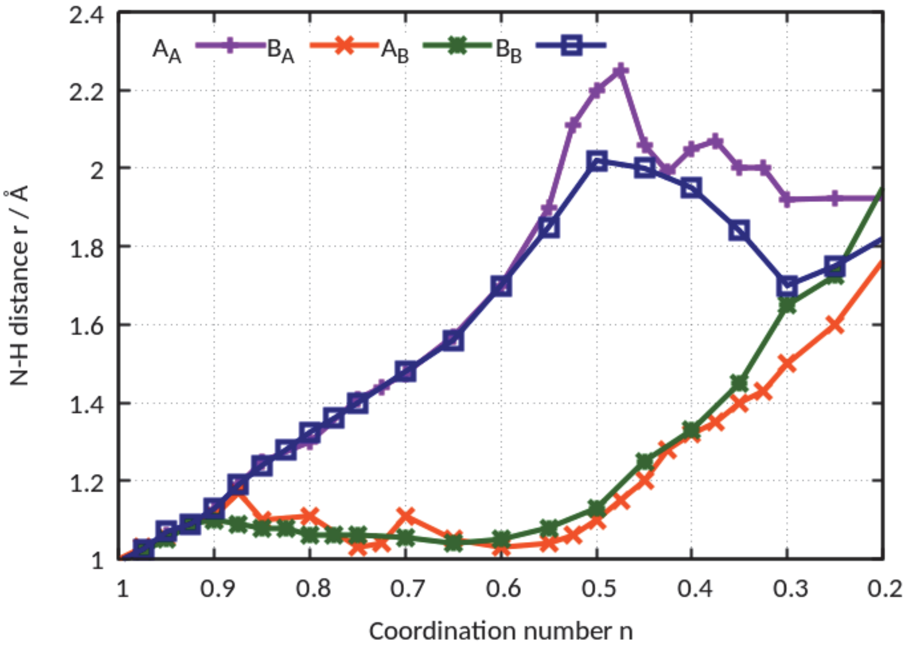

Fig. S14. N–H distance at sites A and B as a function of the coordination number *n* for two different simulations of initially doubly protonated **1**. In one simulation, site A is deprotonated before B (curves A_A and B_A), while in the other site B is deprotonated before A (curves A_B and B_B). The subindex denotes which site deprotonated first. The initial coordination number of n = 1 corresponds to the doubly protonated ligand.

Mass spectra of newly reported oligonucleotides

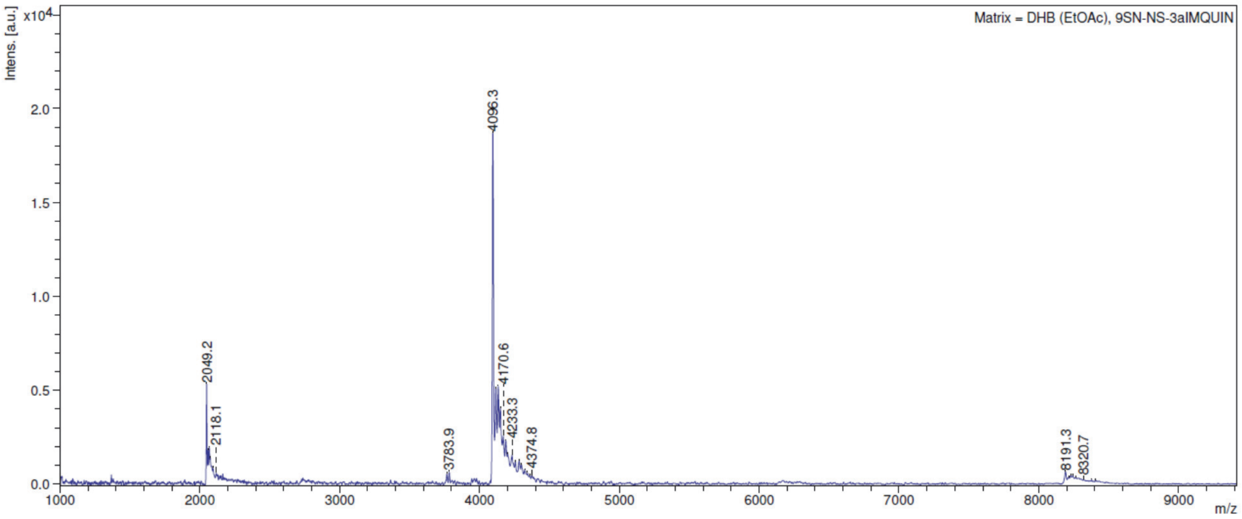

Mass spectrum of ODN1 (calcd. for $(M+H)^+$: 4095 Da)

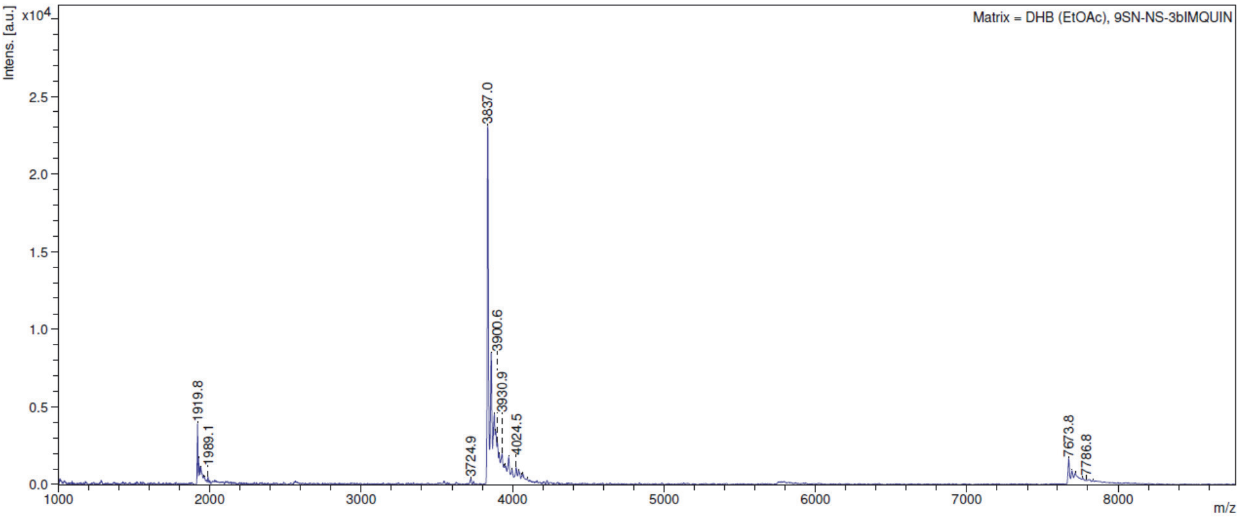

Mass spectrum of ODN2 (calcd. for $(M+H)^+$: 3837 Da)

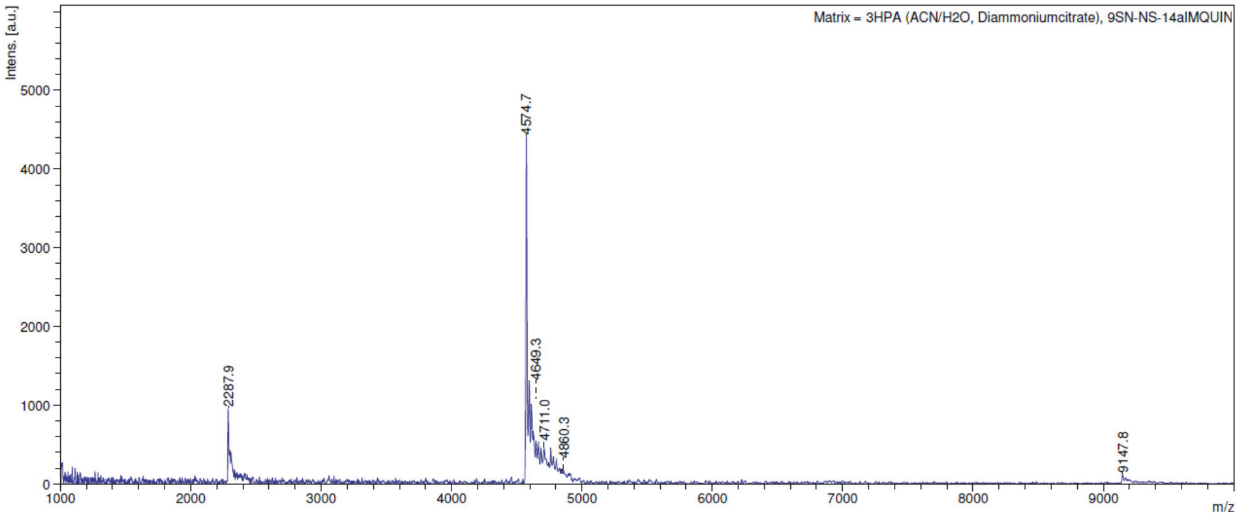

Mass spectrum of ODN7 (calcd. for $(M+H)^+$: 4573 Da)

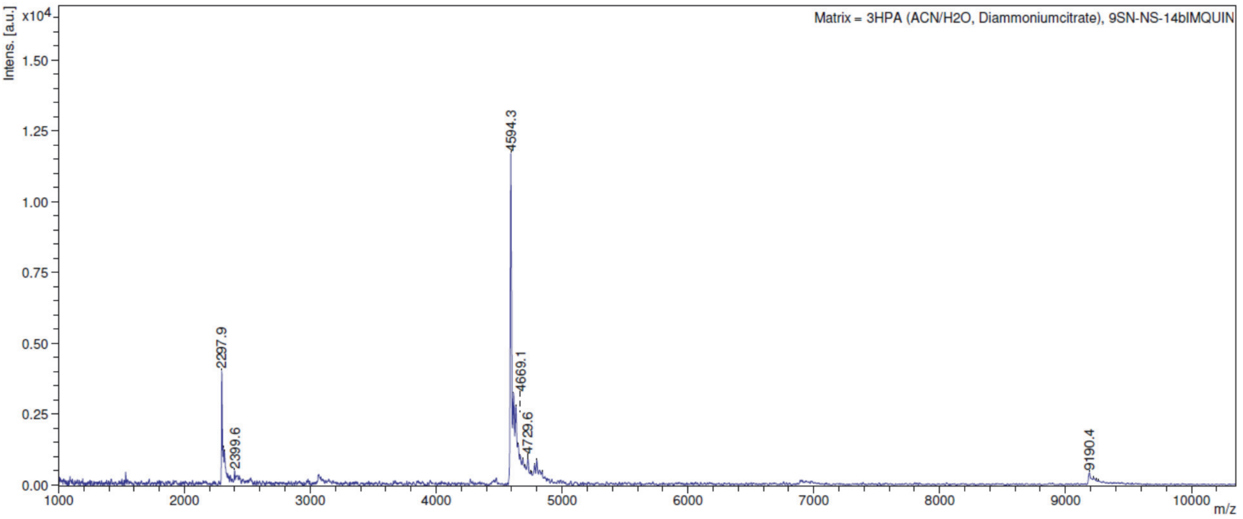

Mass spectrum of ODN8 (calcd. for $(M+H)^+$: 4591 Da)

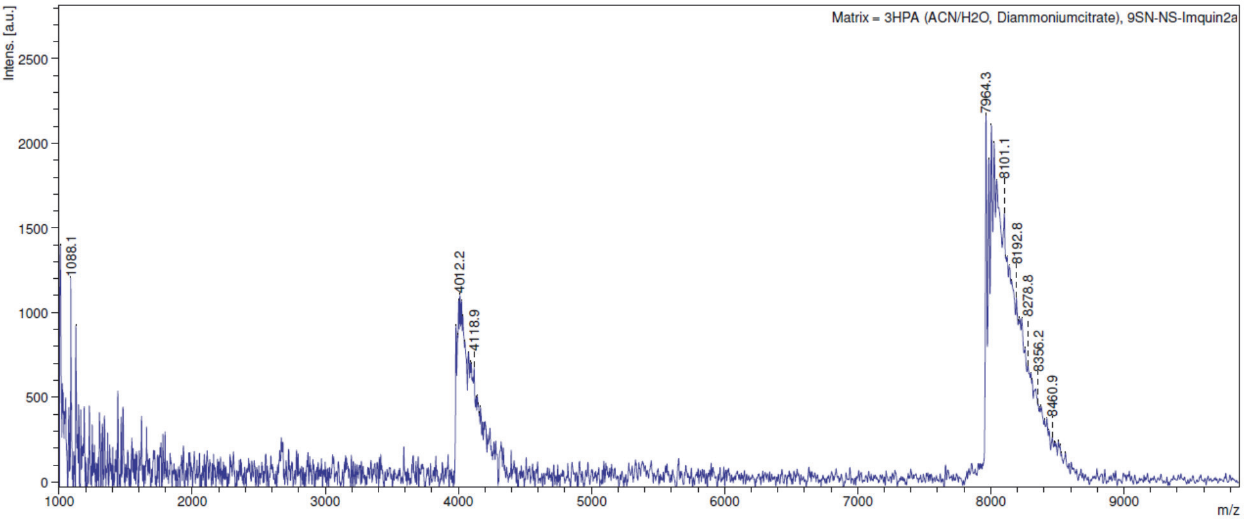

Mass spectrum of ODN13 (calcd. for $(M+H)^+$: 7961 Da)

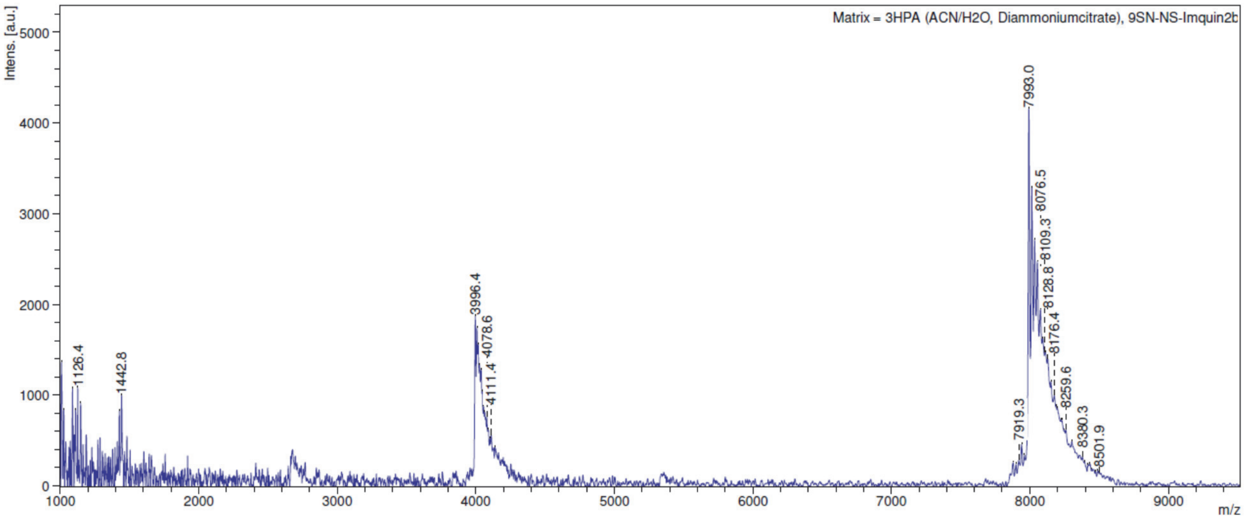

Mass spectrum of ODN14 (calcd. for $(M+H)^+$: 7990 Da)

NMR spectra of newly synthesized compounds

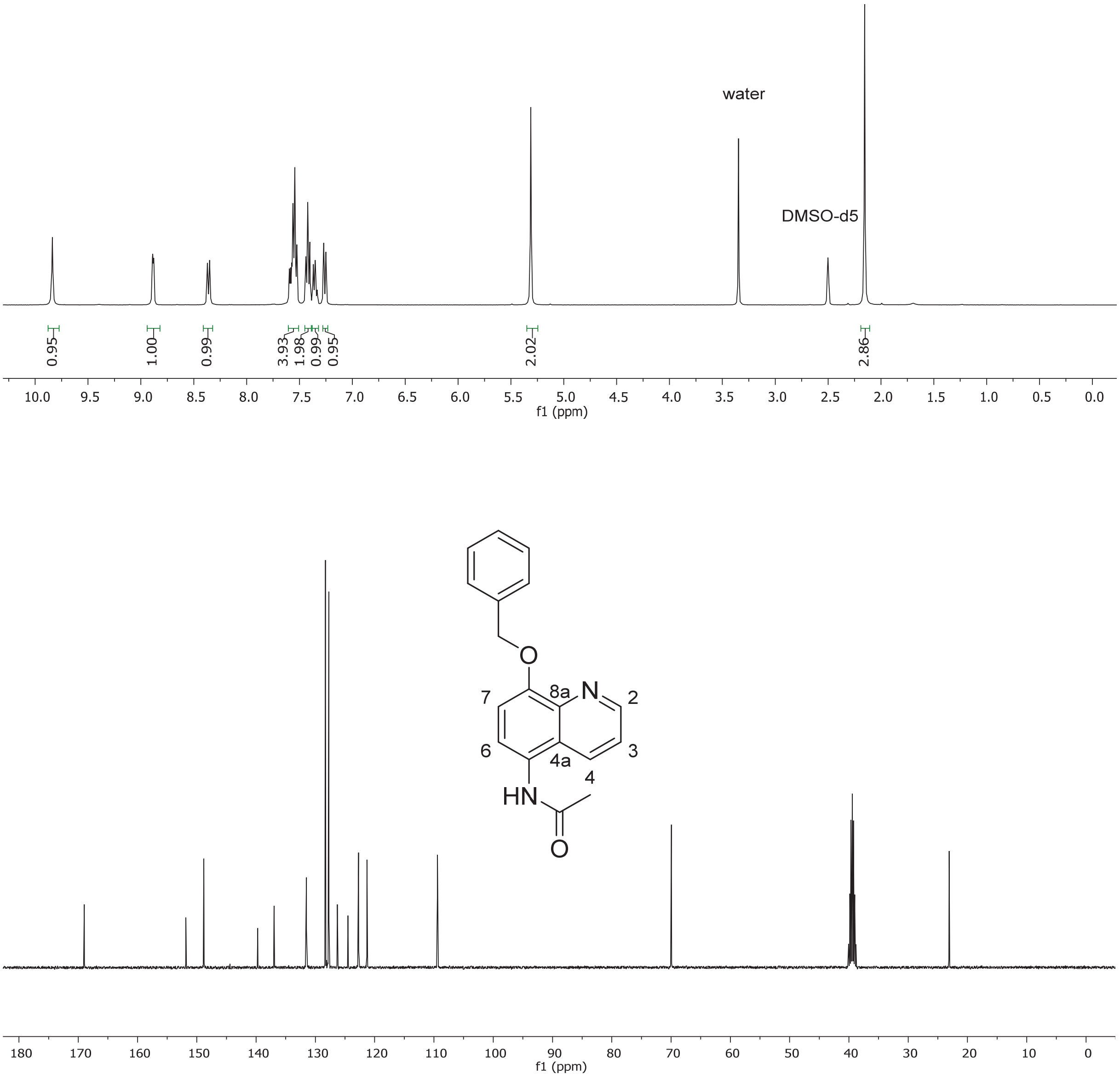

^{1}H and ^{13}C NMR spectra of compound **6** in DMSO-d_6

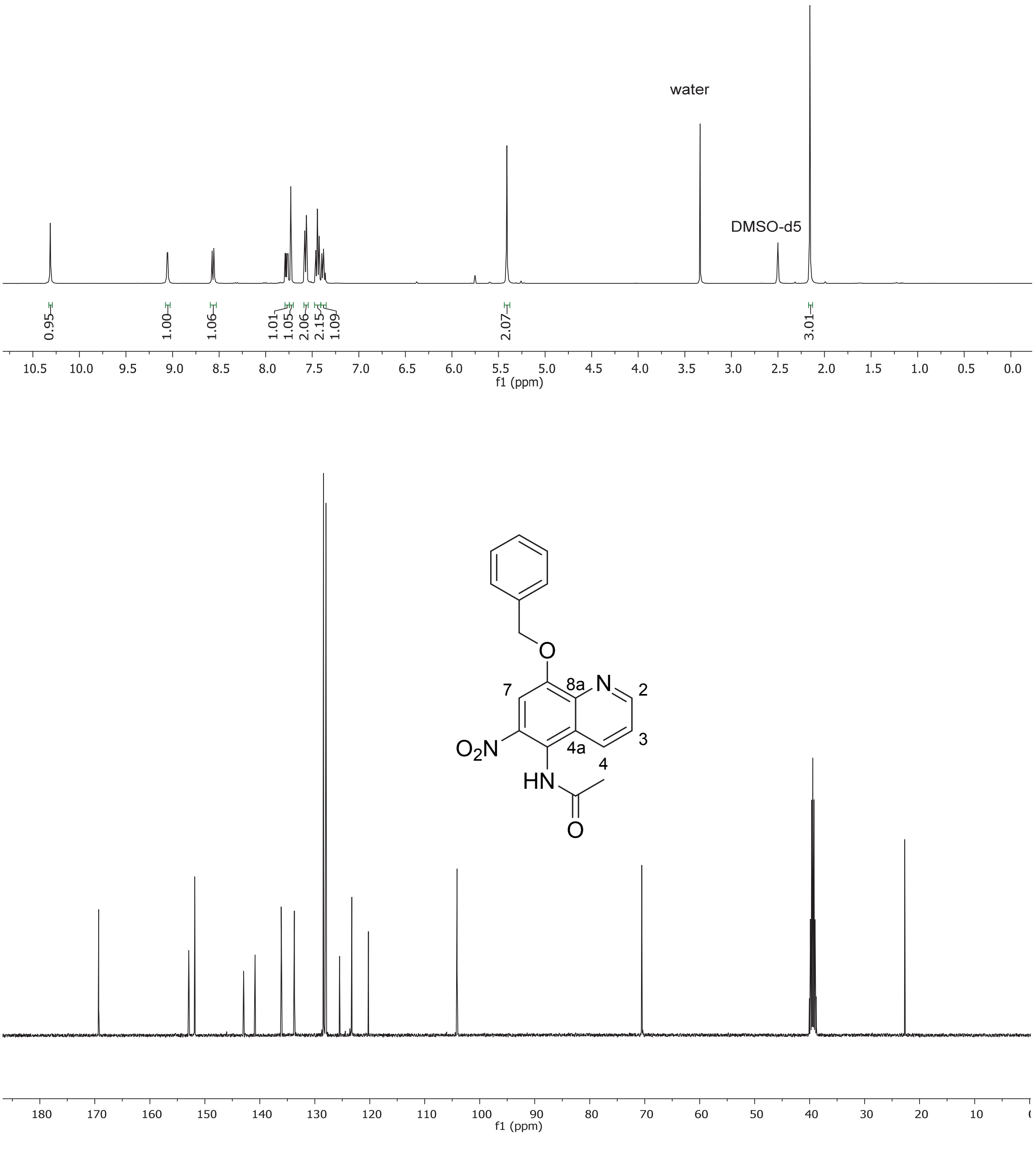

^{1}H and ^{13}C NMR spectra of compound **7** in DMSO-d_6

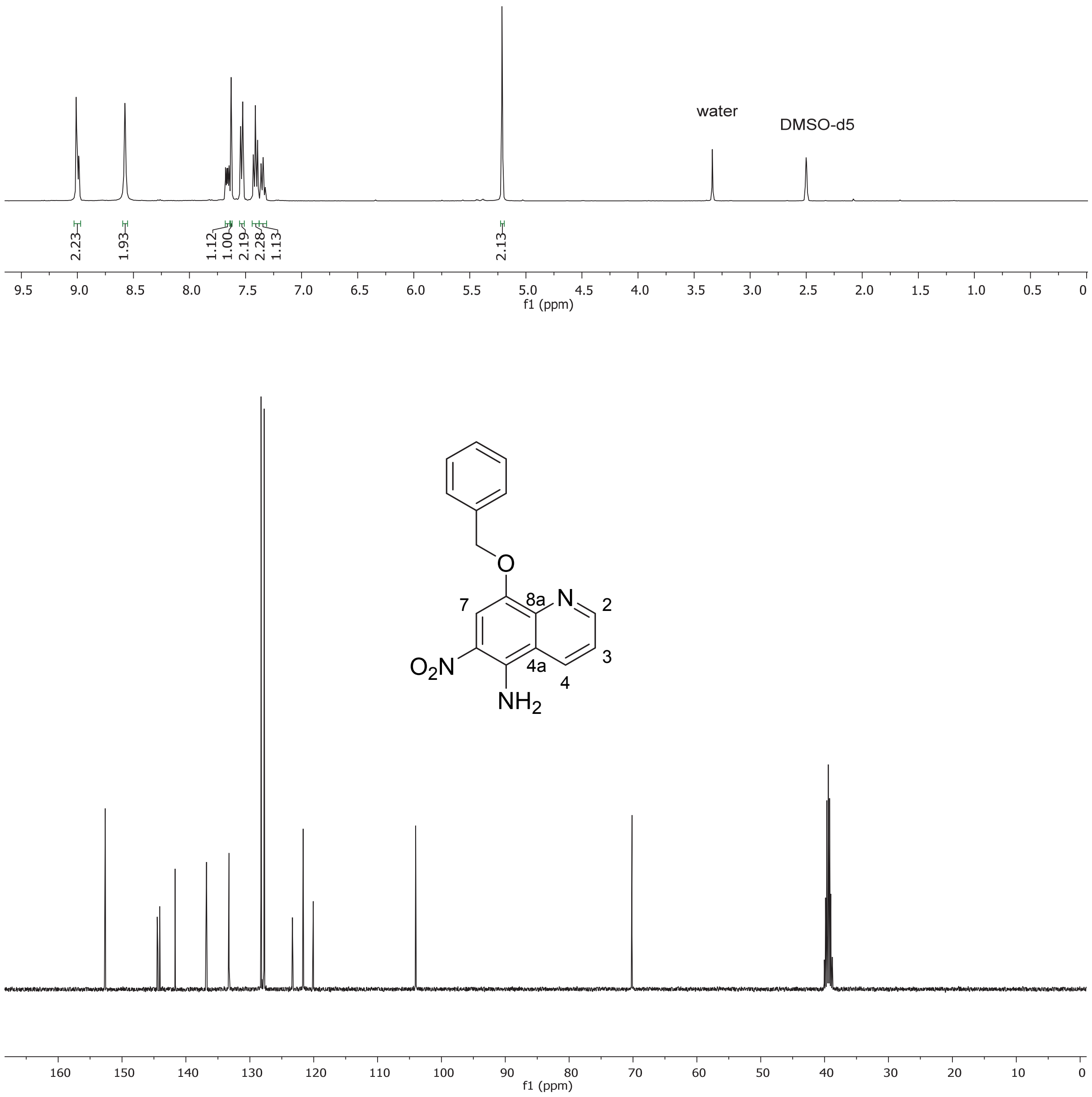

^1H and ^{13}C NMR spectra of compound **8** in DMSO-d_6

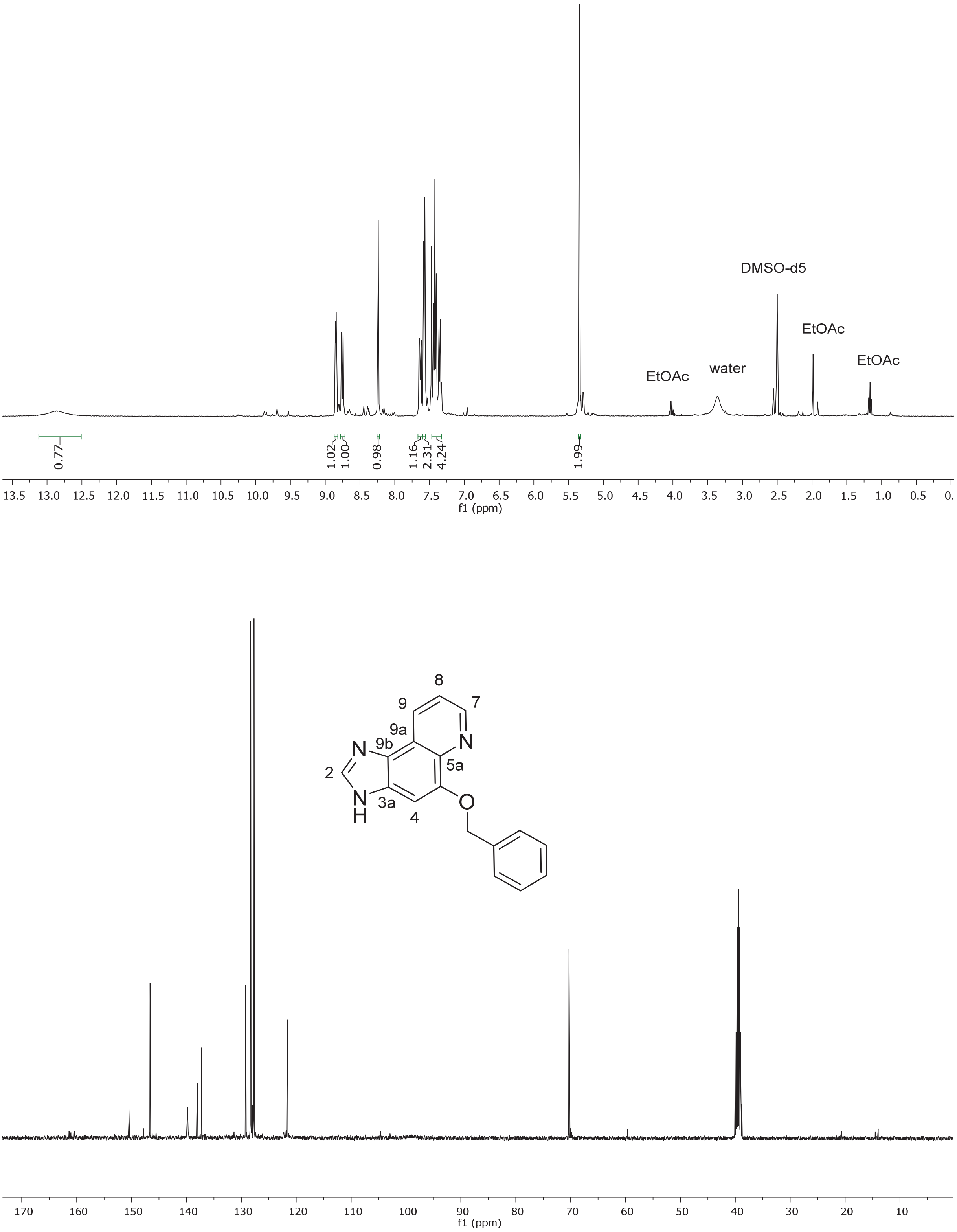

^{1}H and ^{13}C NMR spectra of compound **9** in DMSO-d_6

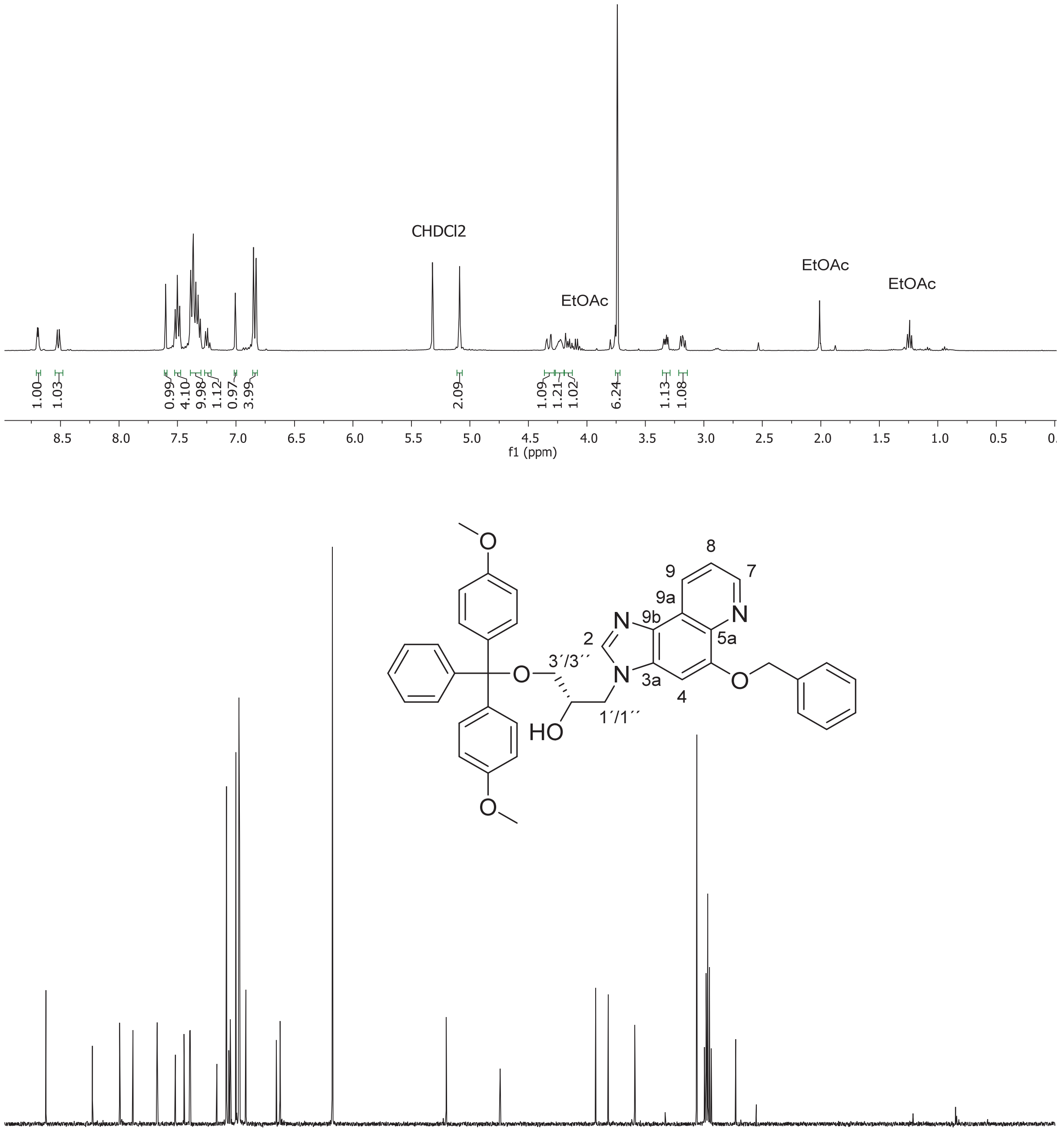

^1H and ^{13}C NMR spectra of compound **10** in CD_2Cl_2

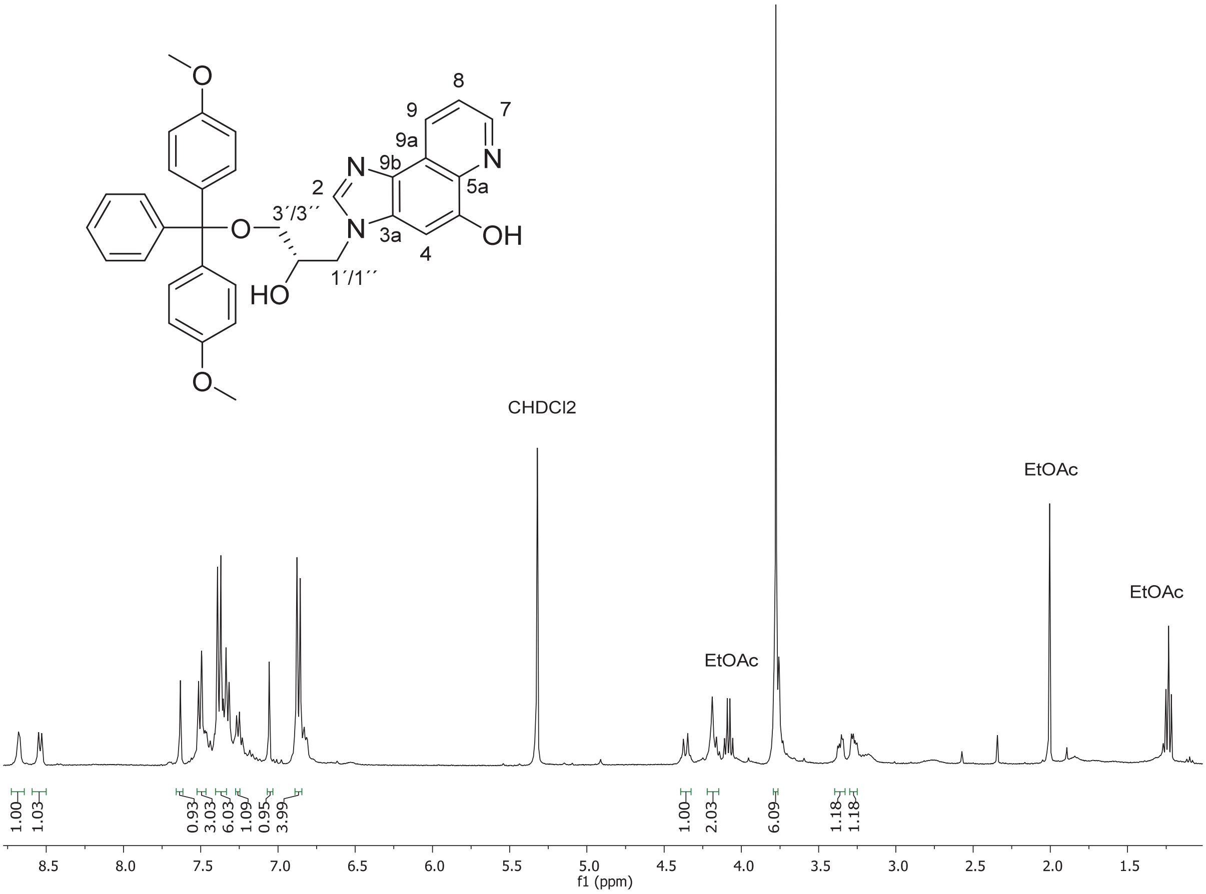

^{1}H NMR spectrum of compound **11** in CD_2Cl_2

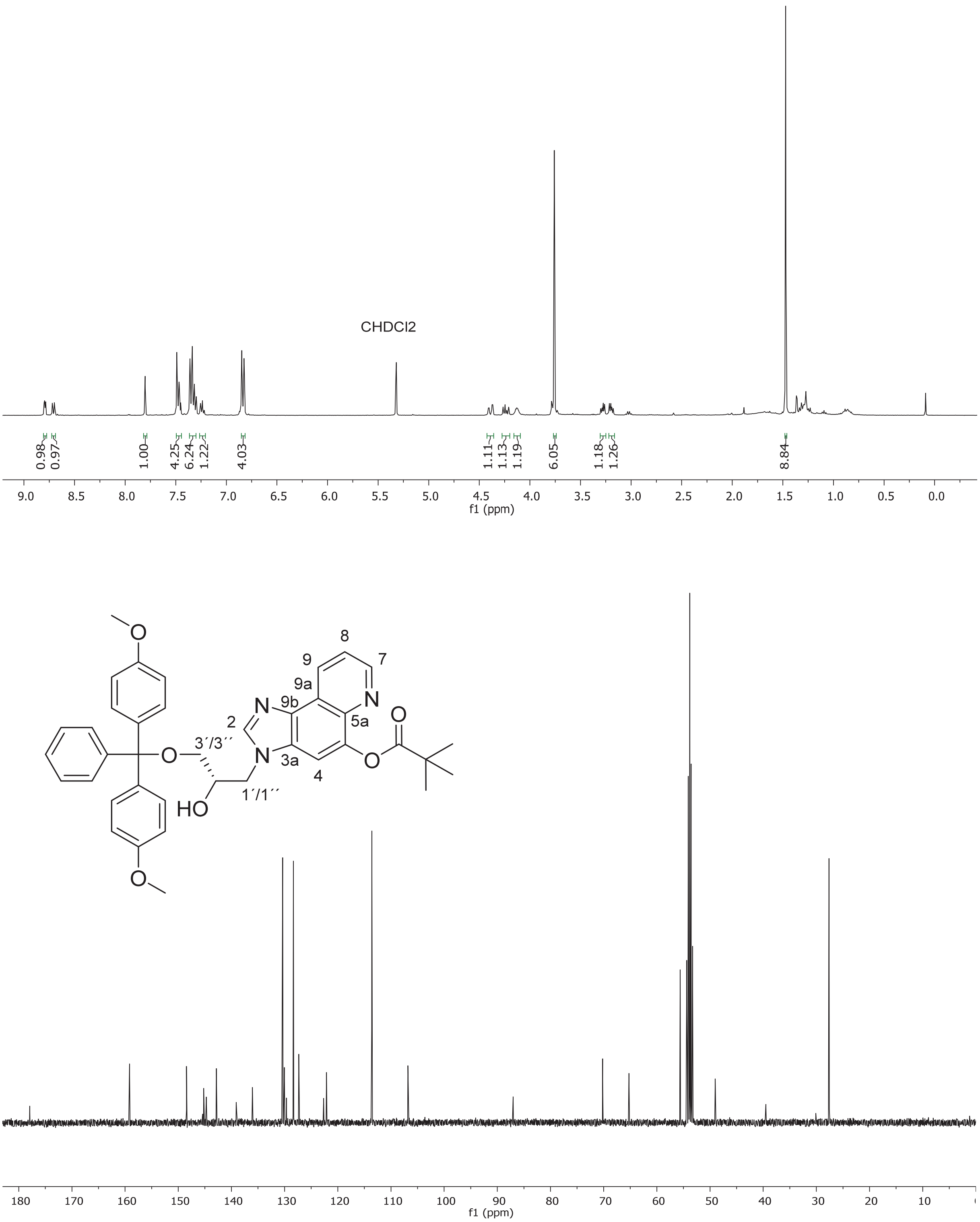

^{1}H and ^{13}C NMR spectra of compound **12** in CD_2Cl_2

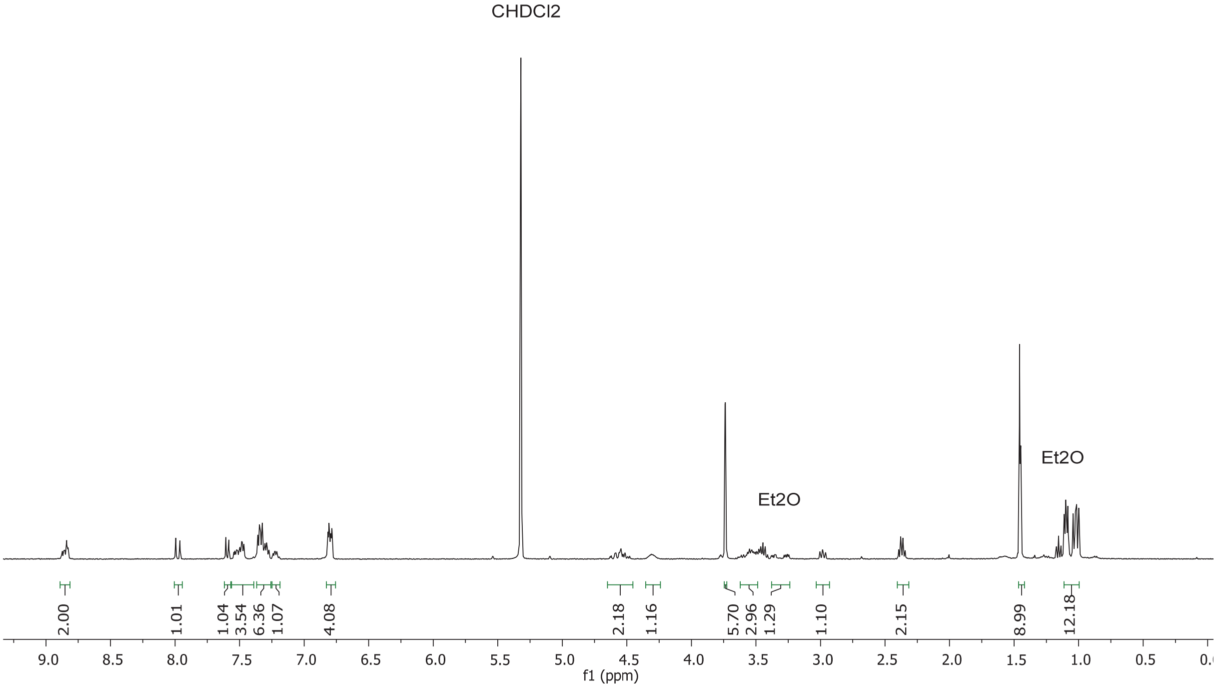

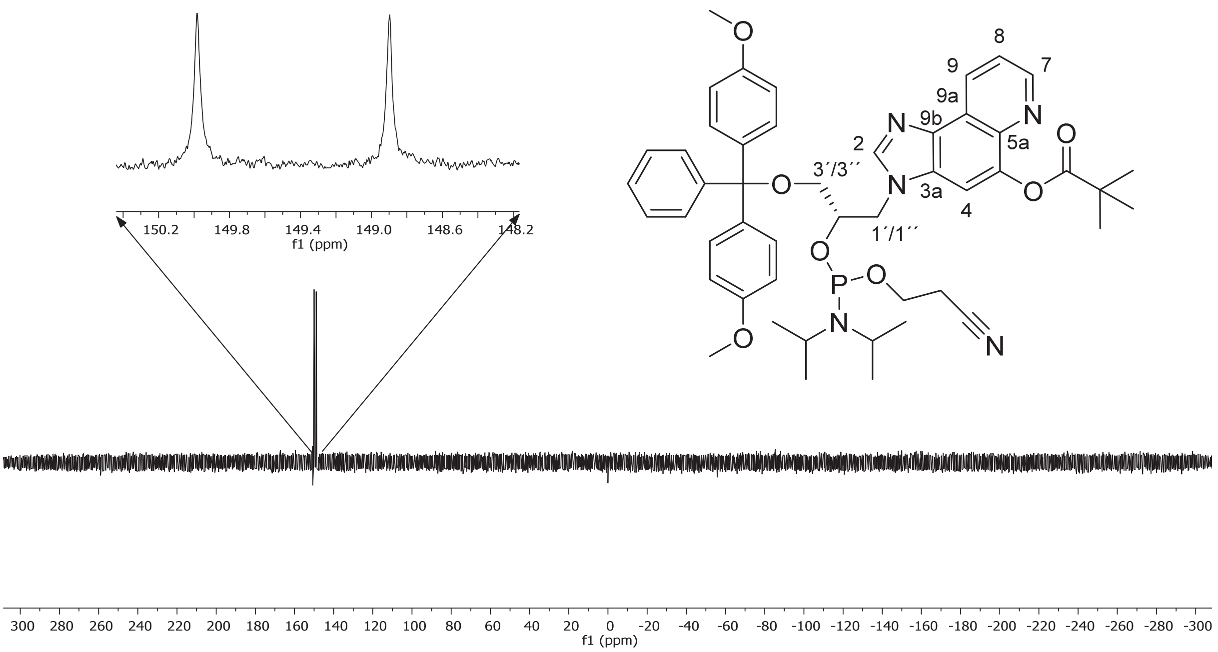

^{1}H and ^{31}P NMR spectra of compound **13** in CD_2Cl_2

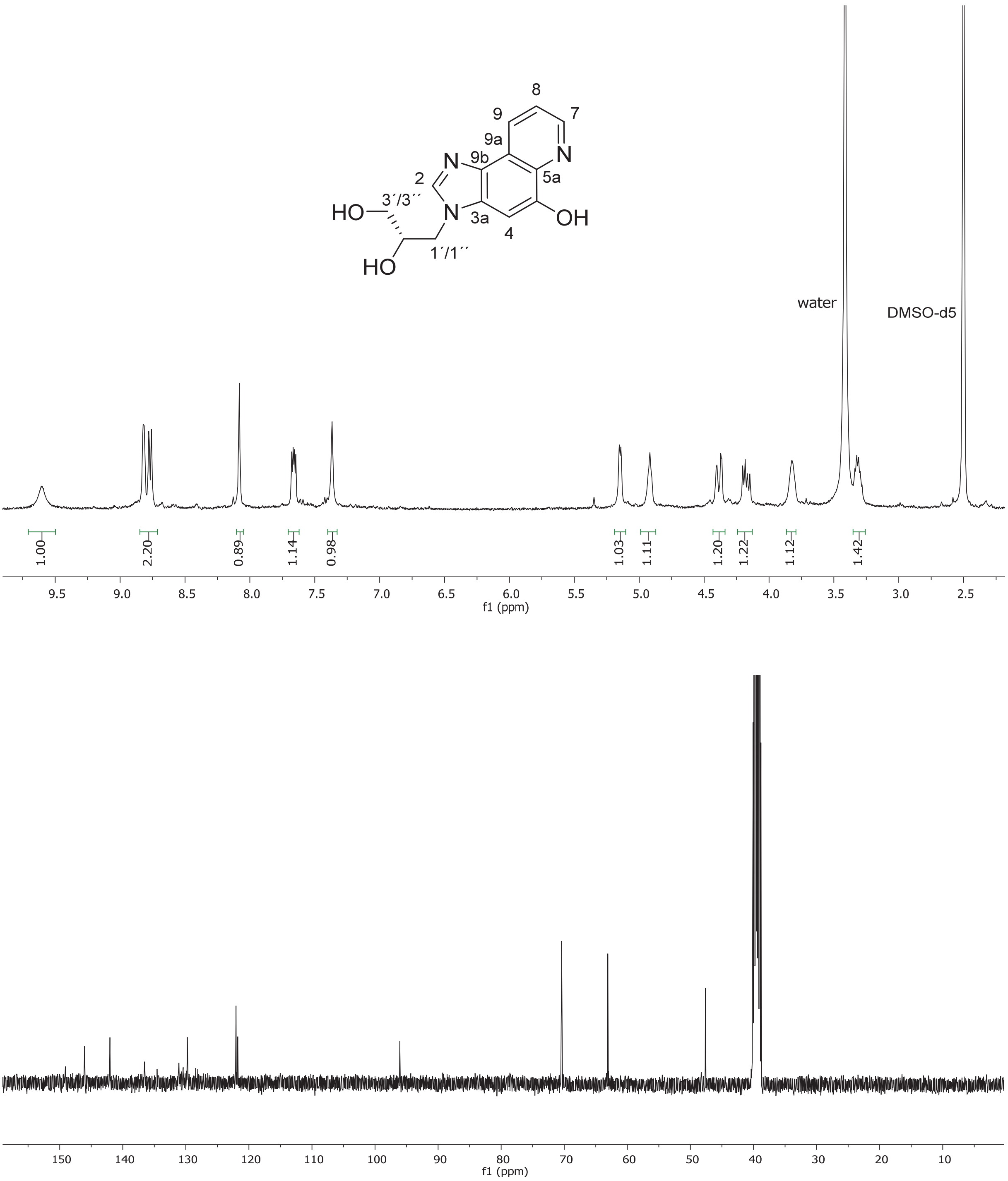

^{1}H and ^{13}C NMR spectra of compound **1** in DMSO-d_6

References

1. N. Sandmann, D. Defayay, A. Hepp and J. Müller, *J. Inorg. Biochem.*, 2019, **191**, 85-93.